Temperature-dependent structural behavior of self-avoiding walks on Sierpinski carpets

Miriam Fritsche,[1] H. Eduardo Roman,[2] and Markus Porto[1]
[1]*Institut für Festkörperphysik, Technische Universität Darmstadt, Hochschulstrasse 8, 64289 Darmstadt, Germany*
[2]*Dipartimento di Fisica, Università di Milano–Bicocca, Piazza della Scienza 3, 20126 Milano, Italy*
(Received 6 August 2007; published 3 December 2007)

We study the temperature-dependent structural behavior of self-avoiding walks (SAWs) on two-dimensional Sierpinski carpets as a simple model of polymers adsorbed on a disordered surface. Thereby, the Sierpinski carpet defines two types of sites with energy 0 and $\epsilon>0$, respectively, yielding a deterministic fractal energy landscape. In the limiting cases of temperature $T\to 0$ and $T\to\infty$, the known behaviors of SAWs on Sierpinski carpets and on regular square lattices, respectively, are recovered. For finite temperatures, the structural behavior is found to be intermediate between the two limiting cases; the characteristic exponents, however, display a nontrivial dependence on temperature.

DOI: 10.1103/PhysRevE.76.061101 PACS number(s): 05.40.−a, 61.41.+e, 61.43.−j

I. INTRODUCTION

The adsorption of polymers on surfaces is important from both a technological and a fundamental point of view. The structural behavior of adsorbed polymers is determined by the interaction with the (usually disordered) surface as well as by intra- and interpolymer interactions. Concerning the latter issue, it is known that linear polymers made of similar monomer units in a good solvent can be accurately modeled by a self-avoiding walk (SAW). A good solvent is a liquid that is able to screen all long-range forces, such that only the short-range (repulsive) interactions remain. Disordered surfaces, on the other hand, are commonly modeled by fractal structures, either deterministic or random ones. Consequently, SAWs in two-dimensional fractals are a well-studied system for polymers adsorbed on surfaces [1,2].

However, despite an intense investigation of the behavior of SAWs in fractals, many theoretically challenging issues remain to be understood. In this paper, we focus our attention on the structural behavior of SAWs in a specific two-dimensional deterministic fractal of infinite ramification, the Sierpinski carpet (see Fig. 1 for a Sierpinski carpet of the second generation). Here, "infinite ramification" refers to the fact that an infinite number of cut operations is required to disconnect any given subset of the structure [3,4]. The behavior of SAWs in these fractal structures has turned out to be quite challenging to understand [5–9]. This is mainly due to the fact that, for infinitely ramified fractal structures, no renormalization group technique is known, in contrast to the case for Sierpinski fractals of finite ramification [10,11]. In fact, a naive generalization of the results known for regular lattices (for which renormalization group techniques are available) yields incorrect estimates, for instance concerning the so-called des Cloizeaux relation [12], which has been shown not to hold for Sierpinski carpets [8,9].

To shed some light on this intriguing model, we study SAWs on Sierpinski carpets in the presence of a finite temperature T. Thereby, the Sierpinski carpet defines sites with energy 0 (the formerly allowed sites) and $\epsilon>0$ (the formerly forbidden sites), yielding a deterministic fractal energy landscape (a related model, in which the forbidden sites remain forbidden but the boundaries between allowed and forbidden sites become attractive, has been studied previously [13]). In the limiting cases of temperature $T\to 0$ and $T\to\infty$, the known behaviors of SAWs on Sierpinski carpets and on regular square lattices, respectively, are recovered. In this energy landscape, the SAW configurations are generated via the reptation algorithm [14,15], with the modification of a finite acceptance probability $\min\{1,\exp(-\Delta E/T)\}$ where ΔE is the energy difference between the attempted and the current configurations. Hence, the reptation algorithm is used here as an importance sampling method which by construction samples mainly the regions in configuration space (that of all possible chain configurations with one chain end located on all available lattice sites) that have large Boltzmann weights and contribute significantly to the observables. The reptation algorithm seems particularly suitable for the present problem, although it is not exact, and allows us to study quite long chains (up to $N=399$, limited by the size of the fractal lattice that can be generated). It should be emphasized that there exist other, relatively more involved, accurate algorithms for studying very long SAW chains, as for instance the method by Berretti and Sokal [16] or the pruned-enriched Rosenbluth method by Grassberger [17].

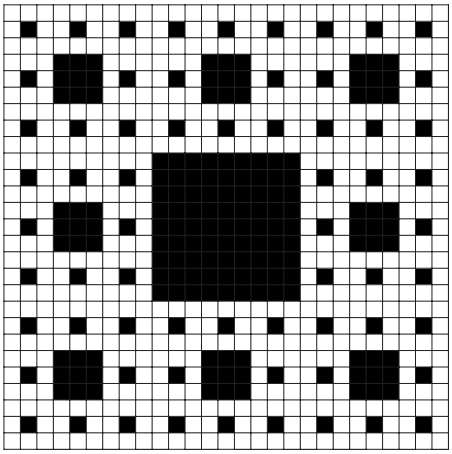

FIG. 1. Illustration of the two-dimensional Sierpinski carpet (also referred to as the Sierpinski square lattice) as obtained after the second iteration. The sites with energy 0 and $\epsilon>0$ are shown as white and black, respectively.

Although these methods can in principle be implemented for our present problem, we consider here the much simpler (constant chain length) reptation approach, which we have shown recently to allow quite accurate estimates for the characteristic exponents describing the probability distribution function (PDF) of the end-to-end distances of SAWs on Sierpinski carpets [9].

The paper is organized as follows: In Sec. II, we define the model we are considering, the quantities of interest, and their scaling functions. The results are discussed in Sec. III, and the conclusions are summarized in Sec. IV.

II. MODEL

We consider a SAW of a fixed number of steps N (i.e., $N+1$ monomers) in a two-dimensional lattice of linear size $L=3\times 3^6=2187$, corresponding to a Sierpinski carpet of the sixth generation (see Fig. 1 for a Sierpinski carpet of the second generation) and apply periodic boundary conditions to minimize boundary effects. The formerly allowed sites are assigned an energy 0, whereas the formerly forbidden sites are assigned an energy $\epsilon>0$. The size of the fractal is chosen such that the largest SAW considered ($N=399$) fits completely into the central square of sites with energy ϵ, even when stretched to a straight line. It is clear that the limiting cases $T\to 0$ and $T\to\infty$ correspond to the cases of SAWs on Sierpinski carpets and on regular square lattices, respectively.

We apply the reptation algorithm to generate SAW configurations, which consists of two steps: (a) picking up at random one of the two ends of the chain, and (b) choosing one of its nearest-neighbor lattice sites at random as its possible new location. If the nearest-neighbor site is empty, the energy difference ΔE between the attempted and current chain configurations is calculated and the reptation step is performed with probability $\min\{1,\exp(-\Delta E/T)\}$, meaning that the whole chain is moved along its track. Otherwise, or if the nearest-neighbor site is occupied, the chain remains at its actual position (in the special case where the occupied nearest-neighbor site corresponds to the other end of the chain, the site is considered empty since it becomes free once the chain moves as a whole). In any case, the process is repeated from step (a) all over again.

To characterize the spatial extension of SAWs in the square lattice, we consider the topological end-to-end distance ℓ after N steps of the walk. The distance ℓ between two points located at coordinates $\{x_1,y_1\}$ and $\{x_2,y_2\}$ is defined as

$$\ell = |x_1 - x_2| + |y_1 - y_2|. \tag{1}$$

The present ℓ metric is equivalent to the more standard Euclidean or r metric [i.e., $r=\sqrt{(x_1-x_2)^2+(y_1-y_2)^2}$], but has the advantage that fluctuations are minimal, permitting a more accurate determination of the characteristic exponents defined below.

The end-to-end distance $\ell(N,T)$ for a given temperature T, averaged over all SAW configurations of N steps, denoted as $\bar{\ell}(N,T)$, obeys the scaling relation [18]

$$\bar{\ell}(N,T) \sim N^{\nu(T)} \quad \text{for } N \gg 1, \tag{2}$$

which defines the possibly temperature-dependent Flory exponent $\nu(T)$. The probability distribution function for the end-to-end distance for a given temperature T, $P(\ell|N,T)$, normalized according to $\int P(\ell|N,T)d\ell=1$, obeys also a scaling form given by

$$P(\ell|N,T) = \frac{2\pi B(T)}{\ell} F\left(\frac{\ell}{\bar{\ell}(N,T)},T\right), \tag{3}$$

where the factor 2π comes from the angular integration and $F(x,T)$ is the temperature-dependent scaling function

$$F(x,T) = \begin{cases} x^{g_1(T)+\tilde{d}(T)} & \text{for } x \ll 1, \\ x^{g_2(T)+\tilde{d}(T)} \exp[-b(T)x^{\delta(T)}] & \text{for } x \gg 1, \end{cases} \tag{4}$$

defining the possibly temperature-dependent characteristic exponents $g_1(T)$, $g_2(T)$, and $\delta(T)$. The effective temperature-dependent fractal dimension $\tilde{d}(T)$ of the substrate, which enters Eq. (4), is given by

$$\tilde{d}(T) = \frac{\ln[8+\exp(-\epsilon/T)]}{\ln 3}, \tag{5}$$

which takes into account that, for finite temperature T, the sites with energy $\epsilon>0$ are accessed with a finite probability $\exp(-\epsilon/T)$, so that, on average, the accessible area $A(\ell,T)$ within some distance ℓ increases as $A(\ell,T)\propto \ell^{\tilde{d}(T)}$. Note that, for $T\to 0$ and $T\to\infty$, the correct fractal dimensions $\tilde{d}(T=0)=\ln 8/\ln 3$ (Sierpinski carpet) and $\tilde{d}(T=\infty)=\ln 9/\ln 3=2$ (regular square lattice) are obtained.

III. RESULTS

We simulate SAWs as described above for various chain lengths N and temperatures T, including the limiting cases $T\to 0$ (corresponding to the Sierpinski carpet) and $T\to\infty$ (corresponding to the regular square lattice). We carefully thermalize the SAW for the desired temperature by a large number of preliminary reptation steps until the mean energy of the chain has reached a plateau and fluctuates around it. Only after that moment are data for the spatial configurations of the chain taken. All resulting SAW configurations are taken into account when performing the statistical average of the end-to-end distance, including those for which no move of the chain has taken place (see, for instance, [15]).

We first analyze the average end-to-end distance $\bar{\ell}(N,T)$ of the SAWs for various chain lengths N and temperatures T according to Eq. (2), yielding, as an average over chain length N, the Flory exponent $\nu(T)$ as a function of temperature T. In Fig. 2, we show $\nu(T)$ vs temperature T, where $\nu(T)\cong 0.75$ is found independent of T. This is consistent with the expected values $\nu(T\to 0)\cong 0.75$ [18] and $\nu(T\to\infty)\cong 0.75$ [8]. Hence, we assume a constant value of $\nu(T)$ in the following.

We proceed with the analysis of the distribution function $P(\ell|N,T)$ with the goal to determine the characteristic expo-

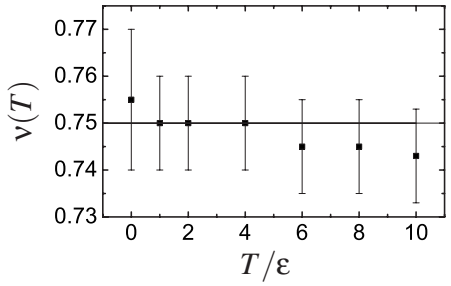

FIG. 2. Plot of the Flory exponent $\nu(T)$ vs temperature T. The behavior is consistent with a temperature-independent value of $\nu(T) \cong 0.75$, shown as the horizontal line. The estimated values are based on simulations for $N=99$, 299, and 399, with the error bars indicating the estimated error. Already, for $T=10$, the behavior of $\bar{\ell}(N,T)$ and hence the value of $\nu(T)$ become indistinguishable from that of the regular square lattice.

nents $g_1(T)$, $g_2(T)$, and $\delta(T)$ as a function of temperature T. In Fig. 3, we exemplify this analysis by showing the distribution function for chain length $N=99$ and three temperatures $T=\infty$ (corresponding to the regular square lattice), ϵ, and 0 (corresponding to the Sierpinski carpet). The value of the characteristic exponent $g_1(T)$ is determined from such plots for various chain lengths N and temperatures T by fitting the part $\ell/N^{\nu(T)} \ll 1$ (the numerical values obtained so

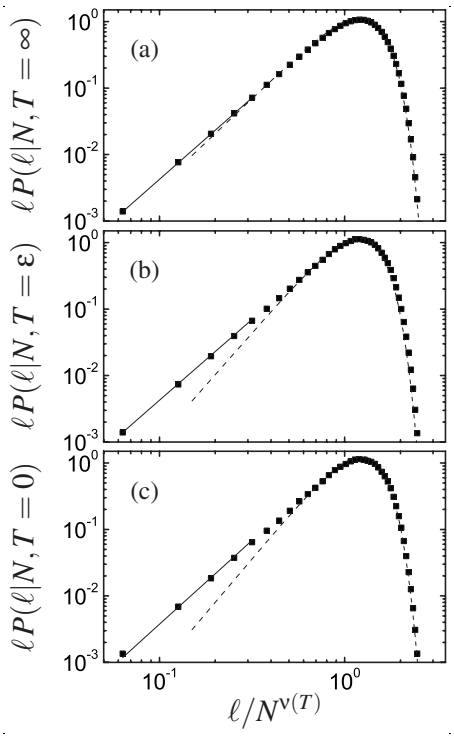

FIG. 3. Plot of the distribution function $\ell P(\ell|N,T)$ vs $\ell/N^{\nu(T)}$, exemplified for $N=99$ and three values of temperature T: (a) $T=\infty$ (regular square two-dimensional lattice), (b) ϵ, and (c) 0 (Sierpinski carpet). The functional form obtained for $\ell/N^{\nu(T)} \ll 1$ [determined by the characteristic exponent $g_1(T)$] is shown as the full line, whereas the functional form for $\ell/N^{\nu(T)} \gg 1$ [determined by the exponents $g_2(T)$ and $\delta(T)$, which are obtained by the ansatz shown in Fig. 4] is displayed as dashed line.

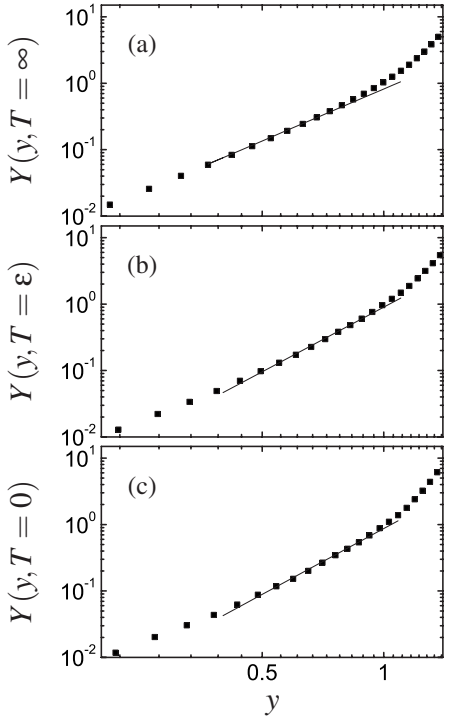

FIG. 4. Plot of the scaling function $Y([b(T)]^{1/\delta(T)}\ell/N^{\nu(T)},T)=[b(T)]^{[g_2(T)+\tilde{d}(T)]/\delta(T)}[B(T)]^{-1}\ell P(\ell|N,T)\exp\{-([b(T)]^{1/\delta(T)}\times\ell/N^{\nu(T)})^{\delta(T)}\}$ vs $y=[b(T)]^{1/\delta(T)}\ell/N^{\nu(T)}$, where $B(T)$ and $b(T)$ are the constants in Eqs. (3) and (4) being determined by the procedure described in Ref. [19] (see main text), exemplified for $N=99$ and three values of temperature T: (a) $T=\infty$ (regular square lattice), (b) ϵ, and (c) 0 (Sierpinski carpet). According to the ansatz, $Y(y,T)$ is expected to scale as $Y(y,T) \propto y^{g_2(T)+\tilde{d}(T)}$ for a properly chosen value of $\delta(T)$, with the fit shown as the full line. The fit is used to obtain the value of $g_2(T)$, and the accuracy is assessed by plotting $X([b(T)]^{1/\delta(T)}\ell/N^{\nu(T)},T)=-\ln\{[b(T)]^{[g_2(T)+\tilde{d}(T)]/\delta(T)}[B(T)]^{-1}\times\ell P(\ell|N,T)([b(T)]^{1/\delta(T)}\ell/N^{\nu(T)})^{-g_2(T)+\tilde{d}(T)}\}$ vs $x=[b(T)]^{1/\delta(T)}\ell/N^{\nu(T)}$, which is expected to scale as $X(x,T) \propto x^{\delta(T)}$.

for different temperatures T are shown below). The characteristic exponents $g_2(T)$ and $\delta(T)$, showing up in the part $\ell/N^{\nu(T)} \gg 1$, need to be determined in a more careful way. Here, we exploit the normalization $\int P(\ell|N,T)d\ell=1$ and the fact that the second moment $\int \ell^2 P(\ell|N,T)d\ell=N^{2\nu(T)}$ to determine the constants $b(T)$ and $B(T)$ in Eqs. (3) and (4), and a scaling function $Y(y,T)$ with $y=[b(T)]^{1/\delta(T)}\ell/N^{\nu(T)}$, which is expected to scale as $Y(y,T) \propto y^{g_2(T)+\tilde{d}(T)}$ for a properly chosen value of $\delta(T)$ (for details of this analysis see [19]). As an example, we show in Fig. 4 the scaling ansatz for chain length $N=99$ and the same three temperatures as in Fig. 3 [the numerical values of $g_2(T)$ and $\delta(T)$ for different temperatures T are shown below].

Using the analysis as exemplified in Figs. 3 and 4, we determine the values for $g_1(T)$, $g_2(T)$, and $\delta(T)$ for various temperatures T as an average over chain length N. The numerical results for $g_1(T)$ and $g_2(T)$ are shown in Fig. 5 and display a nontrivial behavior between the known limiting cases $T \to 0$ (corresponding to the Sierpinski carpet) and $T \to \infty$ (corresponding to the regular square lattice), indicated

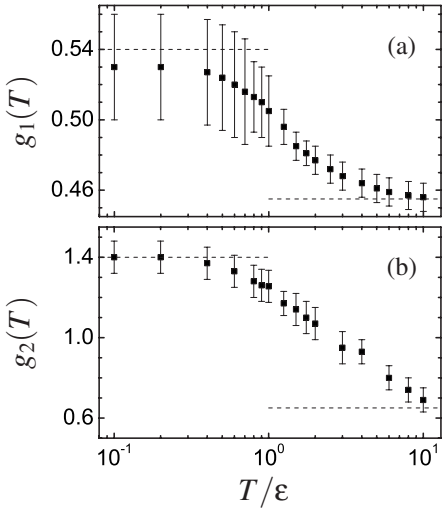

FIG. 5. Plot of the characteristic exponents (a) $g_1(T)$ and (b) $g_2(T)$ vs temperature T. The known limiting cases $T\to 0$ (Sierpinski carpet) and $T\to\infty$ (regular square lattice) are shown as dashed horizontal lines. The estimated values are based on simulations for $N=99$, 299, and 399, with the error bars indicating the estimated error.

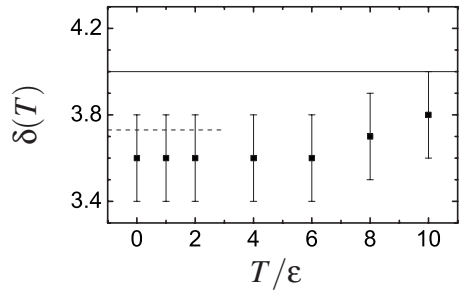

FIG. 6. Plot of the characteristic exponent $\delta(T)$ vs temperature T. The expected value from the Fisher relation [20], $\delta(T)=1/[1-\nu(T)]\cong 4$, and the value $\delta(T=0)=3.73$, which has been found numerically for Sierpinski carpets [8], are shown as full and dashed horizontal lines, respectively. The estimated values are based on simulations for $N=99$, 299, and 399, with the error bars indicating the estimated error.

by dashed lines. Note, in particular, the different shapes, with $g_1(T)$ decreasing significantly earlier as temperature T is increased. This indicates that the probability of compact SAW configurations [which is mainly determined by $g_1(T)$] is much more influenced by a finite temperature T than the probability of SAW configurations of medium size [which is mainly determined by $g_2(T)$].

In Fig. 6, we display the numerically obtained values for $\delta(T)$. It should be noted that the numerical values are below the value expected from the Fisher relation $\delta(T)=1/[1-\nu(T)]$ [20], which gives $\delta(T)\cong 4$ using $\nu(T)\cong 0.75$, independent of T. They are, however, consistent with previous simulations, for instance for Sierpinski carpets [8], which found $\delta(T=0)=3.73\pm 0.30$. Note that the apparent increase of $\delta(T)$ with T cannot be explained by the apparent decrease of $\nu(T)$ with T (cf. Fig. 2), as, according to the Fisher relation, a decreasing $\nu(T)$ would result in a decreasing $\delta(T)$. From our simulations, we conclude that $\delta(T)$ is approximately independent of T, which means that the probability of elongated SAW configurations is not (or hardly) influenced by a finite temperature T.

A crucial issue is whether the observed behavior remains valid in the limit of infinite chain lengths. Since we do numerical simulations, it is never guaranteed that the results do not change in this limit. This question can only be properly addressed by analytical calculations, which, however, do not seem feasible in this case (at least, no such result is known for the Sierpinski carpet, which is in fact the motivation for the present study). In this respect, we have carefully checked, as shown above, that the results do not depend on chain length in the regime of chain lengths that is accessible numerically. Hence, we are confident that the present results will remain valid in the limit of very long chain lengths.

IV. CONCLUSIONS

We study the temperature-dependent structural behavior of self-avoiding walks (SAWs) in two-dimensional Sierpinski carpets as a simple model of polymers adsorbed on a disordered surface. The Sierpinski carpet defines two types of sites, to which we assign energy 0 and $\epsilon>0$, yielding a deterministic fractal energy landscape. We measure the average spatial extension of the SAWs in this energy landscape for various chain lengths N and temperatures T, and determine the characteristic exponents $\nu(T)$, $g_1(T)$, $g_2(T)$, and $\delta(T)$ as functions of temperature T. In the limiting cases of temperature $T\to 0$ and $T\to\infty$, the known behavior of SAWs in Sierpinski carpets and in regular square lattices, respectively, is recovered. For finite temperatures, the structural behavior is found to be intermediate between the two limiting cases, where the characteristic exponents $g_1(T)$ and $g_2(T)$ characterizing the distribution function of the end-to-end distance, however, display a nontrivial dependence on temperature. Since $g_1(T)$ decreases significantly earlier as temperature T is increased, the probability of compact SAW configurations [which is mainly determined by $g_1(T)$] is much more influenced by a finite temperature T than the probability of SAW configurations of medium size [which is mainly determined by $g_2(T)$].

ACKNOWLEDGMENTS

Inspiring discussions with Anke Ordemann are gratefully acknowledged. M.F. thanks C. Riccardi for the warm hospitality at the Physics Department of Università di Milano–Bicocca.

[1] K. Barat and B. K. Chakrabarti, Phys. Rep. **258**, 377 (1995).
[2] *Statistics of Linear Polymers in Disordered Media*, edited by B. K. Chakrabarti (Elsevier, Amsterdam, 2005).
[3] B. B. Mandelbrot, *The Fractal Geometry of Nature* (Freeman, San Francisco, 1982).
[4] Y. Gefen, A. Aharony, and B. Mandelbrot, J. Phys. A **17**, 1277 (1984).
[5] F. D. A. Aarão Reis and R. Riera, J. Stat. Phys. **71**, 453 (1993).
[6] D. Ben-Avraham and S. Havlin, J. Phys. A **16**, L559 (1983).
[7] Y.-h. Taguchi, J. Phys. A **21**, 1929 (1988).
[8] A. Ordemann, M. Porto, and H. E. Roman, J. Phys. A **35**, 8029 (2002).
[9] F. Marini, A. Ordemann, M. Porto, and H. E. Roman, Phys. Rev. E **74**, 051102 (2006).
[10] B. D. Hughes, *Random Walks and Random Environments* (Clarendon Press, Oxford, 1995).
[11] F. A. C. C. Chalub, F. D. A. Aarão Reis, and R. Riera, J. Phys. A **30**, 4151 (1997).
[12] J. des Cloizeaux, Phys. Rev. A **10**, 1665 (1974).
[13] F. D. A. Aarão Reis, J. Stat. Phys. **92**, 659 (1998).
[14] F. T. Wall and F. Mandel, J. Chem. Phys. **63**, 4592 (1975).
[15] F. Mandel, J. Chem. Phys. **70**, 3984 (1979).
[16] A. Berretti and A. D. Sokal, J. Stat. Phys. **40**, 483 (1985).
[17] P. Grassberger, Phys. Rev. E **56**, 3682 (1997).
[18] P. J. Flory, J. Chem. Phys. **17**, 303 (1949).
[19] A. Ordemann, M. Porto, H. E. Roman, S. Havlin, and A. Bunde, Phys. Rev. E **61**, 6858 (2000); note that on p. 6860 of this publication, Ref. [36] should have been quoted in the right column below Eq. (6) instead of the erroneously cited Ref. [30], and that Ref. [30] should have appeared in the discussion of Monte Carlo simulations of SAW on percolation cluster in the lower right column of p. 6861.
[20] M. E. Fisher, J. Chem. Phys. **44**, 616 (1966).